EXTENDED PDF FORMAT
SPONSORED BY
Travel Grants to the
15th International Congress
of Immunology
Apply Now!
R&D SYSTEMS
www.rndsystems.com

Speleothems Reveal 500,000-Year History of Siberian Permafrost

A. Vaks *et al.*

Science **340**, 183 (2013);
DOI: 10.1126/science.1228729

This copy is for your personal, non-commercial use only.

If you wish to distribute this article to others, you can order high-quality copies for your colleagues, clients, or customers by clicking here.

Permission to republish or repurpose articles or portions of articles can be obtained by following the guidelines here.

The following resources related to this article are available online at www.sciencemag.org (this information is current as of April 11, 2013):

Updated information and services, including high-resolution figures, can be found in the online version of this article at:
http://www.sciencemag.org/content/340/6129/183.full.html

Supporting Online Material can be found at:
http://www.sciencemag.org/content/suppl/2013/02/20/science.1228729.DC1.html

This article **cites 28 articles**, 6 of which can be accessed free:
http://www.sciencemag.org/content/340/6129/183.full.html#ref-list-1

This article appears in the following **subject collections:**
Atmospheric Science
http://www.sciencemag.org/cgi/collection/atmos

Downloaded from www.sciencemag.org on April 12, 2013

Science (print ISSN 0036-8075; online ISSN 1095-9203) is published weekly, except the last week in December, by the American Association for the Advancement of Science, 1200 New York Avenue NW, Washington, DC 20005. Copyright 2013 by the American Association for the Advancement of Science; all rights reserved. The title *Science* is a registered trademark of AAAS.

Speleothems Reveal 500,000-Year History of Siberian Permafrost

A. Vaks,[1]* O. S. Gutareva,[2] S. F. M. Breitenbach,[3] E. Avirmed,[4] A. J. Mason,[1] A. L. Thomas,[1] A. V. Osinzev,[5] A. M. Kononov,[2] G. M. Henderson[1]

Soils in permafrost regions contain twice as much carbon as the atmosphere, and permafrost has an important influence on the natural and built environment at high northern latitudes. The response of permafrost to warming climate is uncertain and occurs on time scales longer than those assessed by direct observation. We dated periods of speleothem growth in a north-south transect of caves in Siberia to reconstruct the history of permafrost in past climate states. Speleothem growth is restricted to full interglacial conditions in all studied caves. In the northernmost cave (at 60°N), no growth has occurred since Marine Isotopic Stage (MIS) 11. Growth at that time indicates that global climates only slightly warmer than today are sufficient to thaw extensive regions of permafrost.

Permafrost regions (in which the ground is frozen throughout the year) cover 24% of the Northern Hemisphere land surface and hold ~1700 Gt of organic carbon. When it thaws, permafrost releases CO_2 and CH_4, turning a long-term carbon sink into a source and enhancing the greenhouse effect (*1*, *2*). Permafrost degradation also intensifies thermo-karst development, coastline erosion, and liquefaction of ground previously cemented by ice. The latter endangers infrastructure, including major Siberian oil and gas facilities (*3*). An ability to predict the extent of future permafrost degradation is desirable.

Assessing the response of permafrost to changing climate can be difficult. Instrumental records during the past 20 years indicate substantial warming and thawing of local permafrost conditions (*4*), but permafrost at regional scales is slow to respond to warming, and instrumental records are insufficient to capture the long-term behavior. To understand the long-term response of permafrost to climate change requires knowledge of past permafrost conditions. Dating of organic material (*5*) or ground ice (*6*) can indicate the age of existing permafrost but cannot reveal the longer-term history of permafrost.

Here, we used cave carbonates (speleothems) as a tool to date past permafrost and its relationship to global climate. Vadose speleothems (stalactites, stalagmites, and flowstones) form when meteoric waters (i.e., originating from atmospheric precipitation) seep through the vadose zone into caves. Cave temperatures usually approximate the local mean annual air temperature (MAAT) because of buffering by the surrounding rock (*7*). When cave temperatures drop below 0°C, waters freeze and speleothem growth ceases. Speleothems found in modern permafrost regions are therefore relicts from warmer periods before permafrost formed (*8*–*10*). Absence of water also prevents speleothem growth in arid settings, so speleothem growth episodes in modern deserts are proxies for past wet periods (*11*). Because speleothems can be robustly and precisely dated with U-Th techniques, they provide a detailed history of periods when liquid water was available and when both permafrost and desert conditions were absent.

We reconstructed the history of Siberian permafrost (and the aridity of the Gobi Desert) during the past ~500,000 years, by means of U-Th dating of speleothems in six caves along a north-south transect in northern Asia from Eastern Siberia at 60.2°N to the Gobi Desert at 42.5°N (Fig. 1). The northernmost cave, Lenskaya Ledyanaya, sits today on the boundary of continuous permafrost with MAAT substantially below 0°C (*12*). The permafrost type changes toward the southwest to discontinuous, sporadic, and then permafrost-free conditions (*13*) (Fig. 1). Annual precipitation in this Siberian region is 400 to 600 mm/year, falling mainly during summer. To the south, in the Gobi, MAAT ranges from +2°C to +8°C and little precipitation falls (80 to 200 mm/year) (*14*).

Speleothem thickness provides an indication of long-term liquid water availability along the transect. Only 8 cm of growth is seen in the northernmost cave, increasing to ~70 cm in the

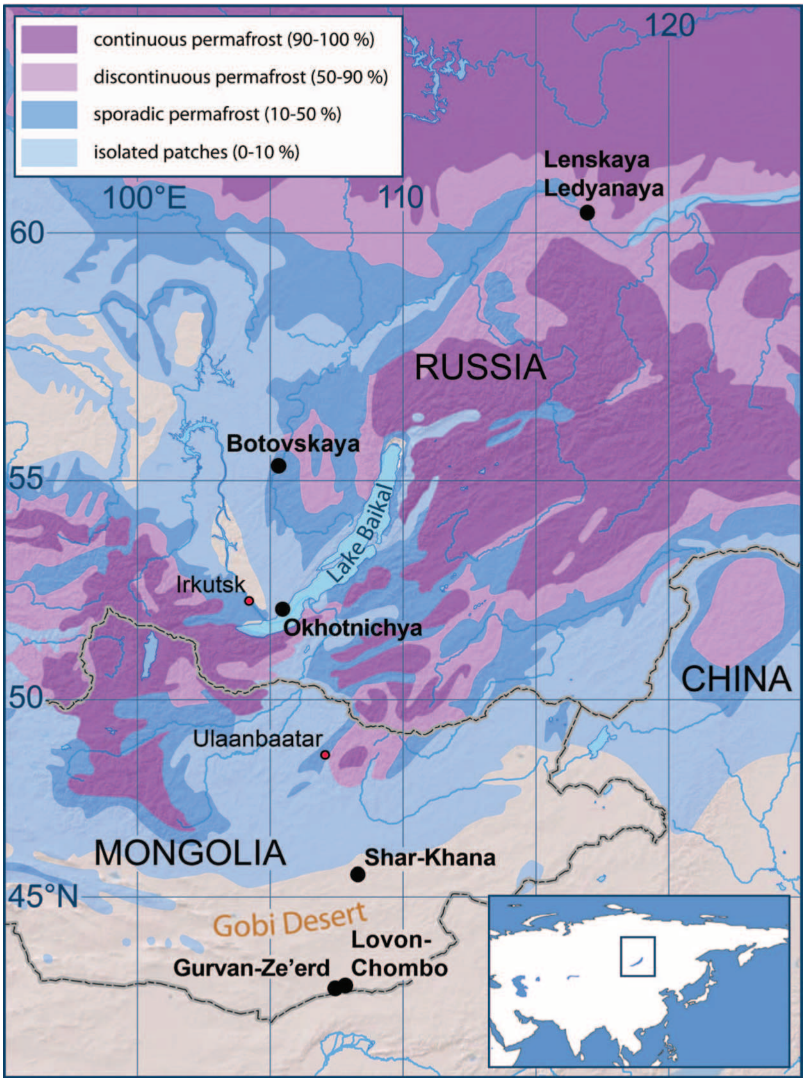

Fig. 1. Map showing the extent of permafrost types in eastern Siberia, the Gobi Desert, and locations of studied caves. Caves are indicated as black circles. [Permafrost data are from (*30*)].

---

[1] Department of Earth Sciences, University of Oxford, Oxford OX1 3AN, UK. [2] Institute of Earth's Crust, Russian Academy of Sciences, Siberian Branch, 128 Lermontova Street, Irkutsk 664033, Russia. [3] Swiss Federal Institute of Technology Zürich (ETH Zürich), CH-8092 Zürich, Switzerland. [4] Institute of Geography, Mongolian Academy of Sciences, 210620 UlaanBaatar, Mongolia. [5] Arabica Speleological Club, Mamin-Sibiryak Street, Box 350, Irkutsk 554082, Russia.

*Corresponding author. E-mail: anton.vaks@earth.ox.ac.uk

caves of southern Siberia and decreasing again to less than 30 cm in the Gobi. As expected, southern Siberia is more suitable for speleothem growth than the cold north or the dry south. All recovered speleothems show a texture of calcium carbonate layers alternating with growth hiatuses (see supplementary materials).

Thirty-six speleothems were collected from the caves, and 111 U-Th ages were determined (Fig. 2A). In each speleothem, at least one sample was taken from the outermost layer and from each section of growth (i.e., between hiatuses) inward, until the limits of the U-Th chronology were reached (age ~500,000 years) to assess all periods of growth. A full description of the samples and their subsampling and dating is given in the supplementary materials.

The youngest speleothem growth in the region of modern continuous permafrost (i.e., at 60°N) occurred during interglacial Marine Isotopic Stage 11 (MIS-11), contrasting with the center of the transect where speleothems grew during all interglacials (Fig. 2, A and B). Age ranges in southern Siberia also demonstrate that the duration of speleothem deposition in MIS-11 was longer than during subsequent interglacials. These observations indicate that permafrost thawing during MIS-11 was more extensive than at any other point during the last 450,000 years and extended northward of 60°N, significantly further north than the present limit of continuous permafrost. Some similar thawing may also have occurred at MIS-13 in this most northerly cave. The absence of any observed speleothem growth since MIS-11 in the northerly Lenskaya Ledyanaya cave, despite dating the outer edges of eight speleothems, suggests the permanent presence of permafrost at this latitude since the end of MIS-11. Speleothem growth in this cave occurred during early MIS-11, ruling out the possibility that the unusual length of MIS-11 caused the permafrost thawing.

MIS-11 was also characterized by wetter conditions in the Mongolian Gobi Desert, as shown by two ages from Shar-Khana Cave speleothems (Fig. 2A), which contrast with the absence of growth during subsequent interglacials. The existence of a humid event in the Gobi during early MIS-11 is supported by mollusk assemblages from the Chinese Loess Plateau (*15*) and by the dominance of input into Lake Baikal via the Selenga River during MIS-11 (*16*).

The degradation of permafrost at 60°N during MIS-11 allows an assessment of the warming required globally to cause such extensive change in the permafrost boundary. There is compelling evidence that MIS-11 was the warmest of recent interglacials, including the presence of boreal forest on South Greenland at that time (*17*), the absence of ice-rafted debris in the North Atlantic (*18*), increased sea levels (*19*), and higher sea surface temperatures (SSTs) in the tropical Pacific (*20*–*22*). Mg/Ca reconstructions (*21*, *22*) indicate that the SST of the Pacific Warm Pool (PWP) reached >30°C in early MIS-11, compared to 29.5°C in MIS-5.5 and ~28.5°C during the pre-industrial Late Holocene (Fig. 2D). This tropical heat was transported poleward (*23*), and there is evidence of unusual warmth in Siberia during MIS-11, evidenced by the high fraction of biogenic silica in the sediments of Lake Baikal (*24*) (Fig. 2C) and high spruce pollen content in Lake El'gygytgyn, suggesting local temperatures 4° to 5°C above the present (*25*). When PWP

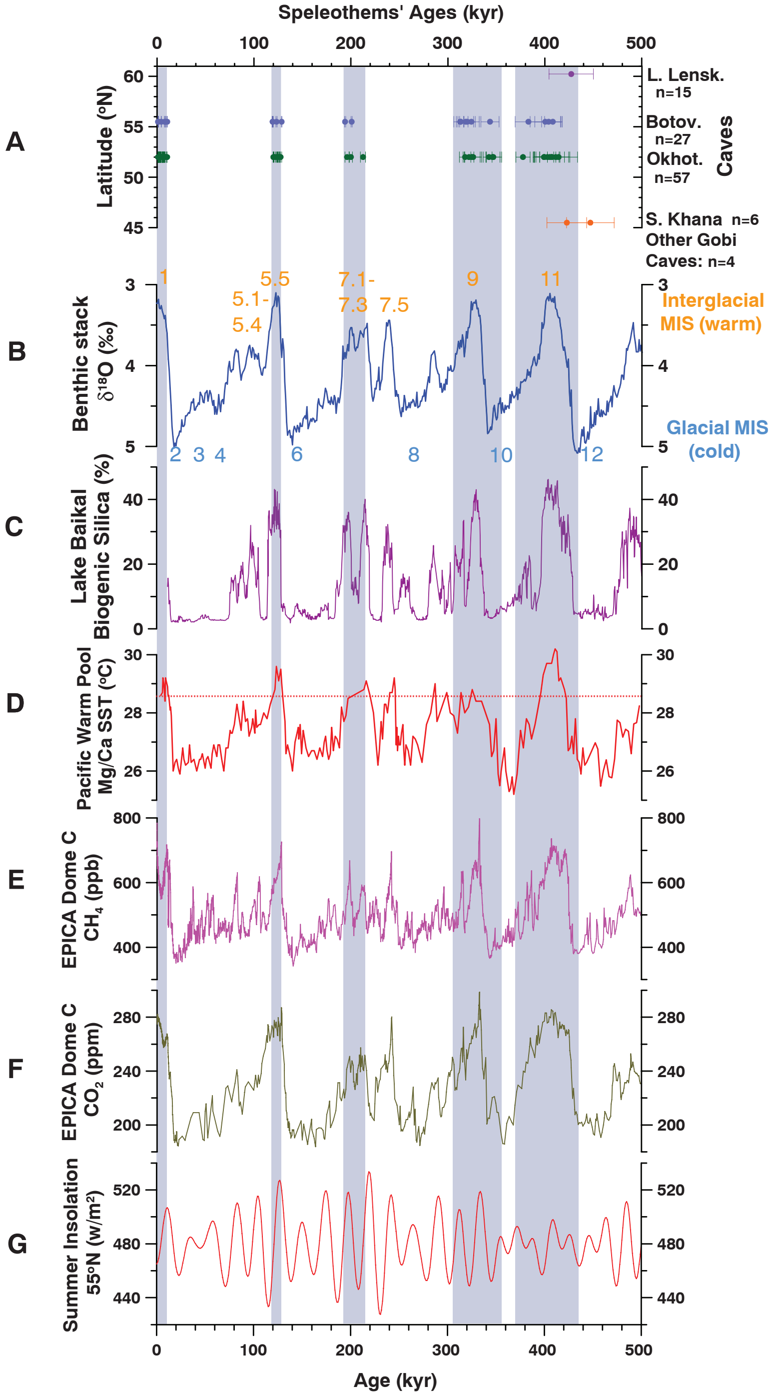

Fig. 2. Comparison of speleothems' growth periods in Siberia and Mongolia with other paleoclimate records of the past 500,000 years. Gray vertical bars indicate periods of growth in Okhotnichya and Botovskaya caves. (**A**) Distribution of speleothem U-Th ages [in thousands of years (kyr); ±2σ] in time and space; *n* = total number of U-Th age determinations per cave, including those beyond the U-Th range. (**B**) Benthic δ^{18}O stack (*31*) with MIS numbers. (**C**) Concentration of biogenic silica in Lake Baikal sediments (*24*). (**D**) Pacific Warm Pool Mg/Ca SST, with the pre-industrial Late Holocene SST shown by red horizontal fragmented line (*21*, *22*). (**E** and **F**) CH_4 and CO_2 records, respectively, of EPICA Dome C (*26*, *27*). (**G**) Summer insolation at 55°N (*29*). Speleothems with ages exceeding 500,000 years (within ±2σ range) are not shown in (A) but are accounted for in *n*. Two samples, SLL9-2-A+B and SOP-32-B, are not included because they reflect a mixture of material from different layers; see table S1.

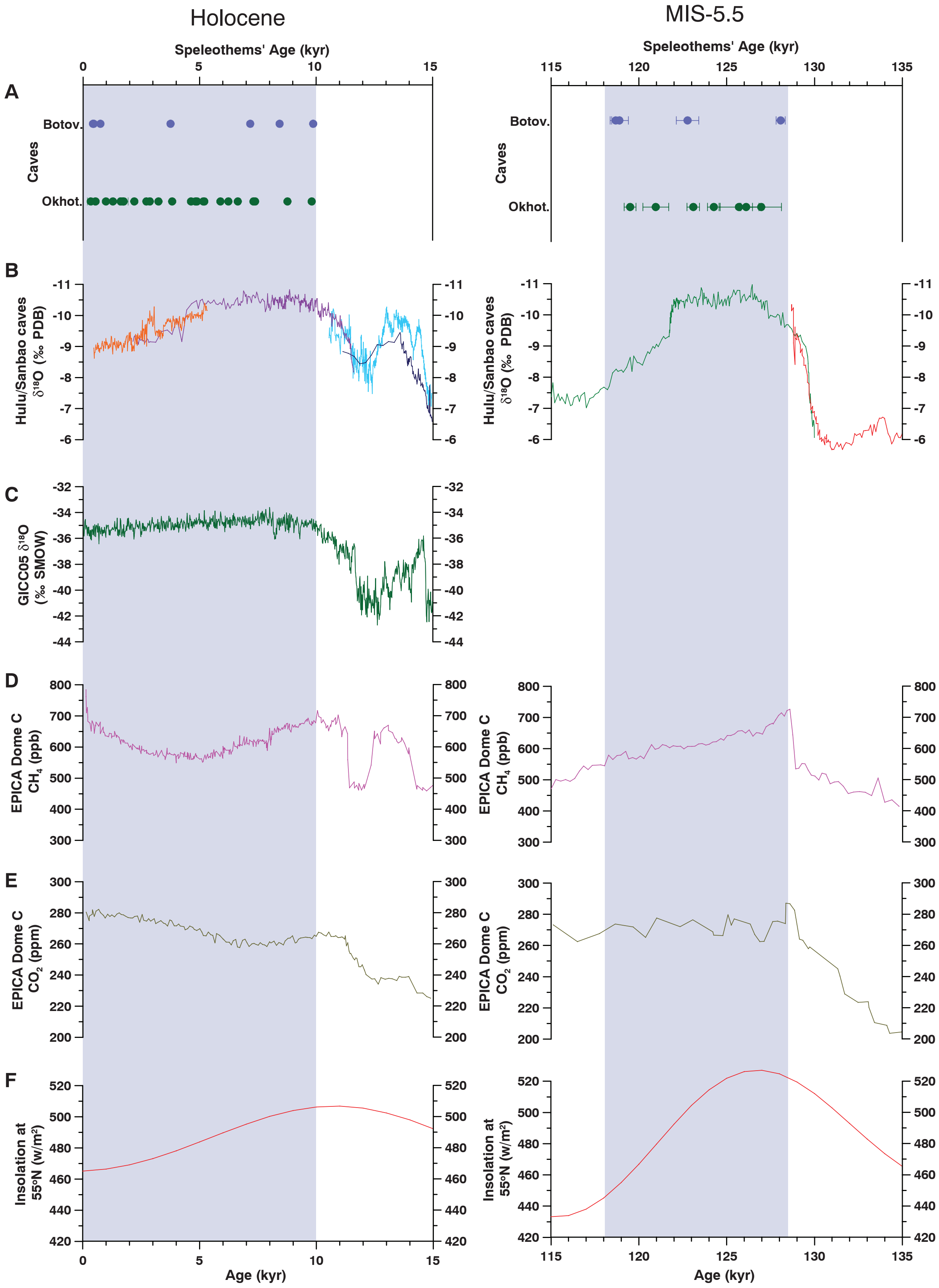

Fig. 3. Comparison of MIS-5.5 and Holocene speleothems' growth periods with other paleoclimate records. Gray vertical bars indicate periods of growth. (**A**) Siberian speleothem growth periods during the Holocene and MIS-5.5. (**B**) East Asian monsoon records from Hulu and Sanbao caves (*32*). (**C**) GICC05 $\delta^{18}O$ (*33*, *34*). (**D** and **E**) CH_4 and CO_2 records, respectively, of EPICA Dome C (*26*, *27*). (**F**) Summer insolation at 55°N (*29*).

temperatures reached 30°C, this appears to have caused more pronounced warming of northern continents and to have led to substantial northward migration of the permafrost boundary.

Periods of Siberian speleothem growth since MIS-11 suggest a close link between greenhouse warming (hence global temperatures) and permafrost extent. After a brief hiatus in growth after MIS-11 (from 370,000 to 355,000 years ago), coinciding with a minimum in atmospheric CO_2 and in PWP SST during MIS-10 (Fig. 2, D and F), large thicknesses of speleothem grew in Southern Siberia during MIS-9 as greenhouse gases returned to higher values. Speleothems also grew actively during MIS-5.5 and the Holocene (>5 cm) when CO_2 levels were high. In contrast, growth during MIS-7, a period of lower CO_2 and cooler global conditions, is minimal (maximum 1.5 cm in any studied cave), and no growth is observed during MIS-5.4 to 5.1. Conditions during MIS-7 were at the very limit for growth in southern Siberia: Speleothems grew during MIS-7.3 and 7.1 in Okhotnichya Cave (52°N) but only during MIS-7.1 just to the north at Botovskaya Cave (55°N). No growth occurred during MIS-7.5 at either cave despite higher concentrations of CO_2 and CH_4 than later in MIS-7 (*26*, *27*) and high PWP SST (Fig. 2, D to F) (*21*, *22*). Lake Baikal biogenic silica (*24*) and the percentage of arboreal pollen in Lake El'gygytgyn sediments (*28*) are also lower during MIS-7.5 than during MIS-7.3 and 7.1. Lower local summer insolation during MIS-7.5 (Fig. 2G) (*29*) suggests a role for local insolation in overprinting a Siberian climate dominantly controlled by global greenhouse gas levels.

U-Th dating of Siberian speleothem growth during recent interglacials allows detailed comparison of permafrost history with other aspects of the global climate system (Fig. 3). During MIS-5.5, speleothems started growing between 128,700 and 127,300 years ago, and this growth ended between 119,200 and 118,100 years ago (as determined from Bayesian analysis of U-Th data using OxCal-4.1; see supplementary materials). The permafrost thawing initiated when insolation was close to its maximum and greenhouse gases had just reached maximum values. Holocene permafrost degradation at our sites lags maximum insolation and greenhouse gas concentrations slightly, and starts between 10,000 and 9800 years ago. This lag may be due to the time required for permafrost to thaw at the slightly lower insolation and CO_2 levels of the Holocene (relative to MIS-5.5).

Overall, dated periods of speleothem growth allow an assessment of the relationship between global temperature and permafrost extent. PWP SST was 0.5° to 1.0°C higher during MIS-5.5 and ~1.5°C higher during early MIS-11 relative to the pre-industrial Late Holocene (Fig. 2D) (*21*, *22*). Using PWP SST as a surrogate for global temperature (*21*) suggests that an increase in global temperatures by 0.5° to 1.0°C will degrade only noncontinuous permafrost in southern Siberia, with the Gobi Desert remaining arid. Warming of ~1.5°C (i.e., as in MIS-11) may cause a substantial thaw of continuous permafrost as far north as 60°N and may create wetter conditions in the Gobi Desert. Such warming is therefore expected to markedly change the environment of continental Asia and can potentially lead to substantial release of carbon trapped in the permafrost into the atmosphere.

References and Notes

1. G. Grosse *et al.*, *EOS* **92**, 73 (2011).
2. E. A. G. Schuur *et al.*, *Bioscience* **58**, 701 (2008).
3. O. Anisimov, S. Reneva, *AMBIO* **35**, 169 (2006).
4. V. E. Romanovsky, S. L. Smith, H. H. Christiansen, *Permafr. Periglac. Proc.* **21**, 106 (2010).
5. Y. K. Vasil'chuk, J.-C. Kim, A. C. Vasil'chuk, *Nucl. Instrum. Methods Phys. Res. B* **223–224**, 650 (2004).
6. D. A. Gilichinsky *et al.*, *Quat. Sci. Rev.* **26**, 1547 (2007).
7. H. P. Schwarcz, in *Handbook of Environmental Isotope Geochemistry*, P. Fritz, J. C. Fontes, Eds. (Elsevier, Amsterdam, 1986), vol. 2, pp. 271–300.
8. R. A. Cliff, C. Spötl, A. Mangini, *Quat. Geochronol.* **5**, 452 (2010).
9. B. Lauriol, D. C. Ford, J. Cinq-Mars, W. A. Morris, *Can. J. Earth Sci.* **34**, 902 (1997).
10. S. E. Lauritzen, *Quat. Res.* **43**, 133 (1995).
11. A. Vaks, M. Bar-Matthews, A. Matthews, A. Ayalon, A. Frumkin, *Quat. Sci. Rev.* **29**, 2647 (2010).
12. *Philip's Modern School Atlas, 95th Edition* (Philip's/Octopus, London, 2007).
13. A. Jones *et al.*, Eds., *Soil Atlas of the Northern Circumpolar Region* (Publication Office of the European Union, Luxembourg, 2010).
14. D. Dorjotov, N. Orshikh, T. Oyunchimeg, *Geographic Atlas of Mongolian Republic* (Mongolian Institute of Geodesy and Cartography, Ulaanbaatar, 2004). [in Mongolian]
15. N. Wu *et al.*, *Quat. Sci. Rev.* **26**, 1884 (2007).
16. A. W. Mackay *et al.*, *J. Quat. Sci.* **23**, 365 (2008).
17. A. de Vernal, C. Hillaire-Marcel, *Science* **320**, 1622 (2008).
18. J. F. McManus, D. W. Oppo, J. L. Cullen, *Science* **283**, 971 (1999).
19. M. E. Raymo, J. X. Mitrovica, *Nature* **483**, 453 (2012).
20. L. Ortlieb, A. Diaz, N. Guzman, *Quat. Sci. Rev.* **15**, 857 (1996).
21. J. Hansen *et al.*, *Proc. Natl. Acad. Sci. U.S.A.* **103**, 14288 (2006).
22. M. Medina-Elizalde, D. W. Lea, *Science* **310**, 1009 (2005).
23. A. J. Dickson *et al.*, *Nat. Geosci.* **2**, 428 (2009).
24. A. A. Prokopenko *et al.*, *Quat. Res.* **55**, 123 (2001).
25. M. Melles *et al.*, *Science* **337**, 315 (2012).
26. L. Loulergue *et al.*, *Nature* **453**, 383 (2008).
27. D. Lüthi *et al.*, *Nature* **453**, 379 (2008).
28. N. R. Nowaczyk *et al.*, *Geophys. J. Int.* **150**, 109 (2002).
29. J. Laskar *et al.*, *Astron. Astrophys.* **428**, 261 (2004).
30. J. Brown, O. J. Ferrians Jr., J. A. Heginbottom, E. S. Melnikov, *Circum-Arctic Map of Permafrost and Ground Ice Conditions* (National Snow and Ice Data Center/World Data Center for Glaciology, Boulder, CO, 2001).
31. L. E. Lisiecki, M. E. Raymo, *Paleoceanography* **20**, PA1003 (2005).
32. Y. Wang *et al.*, *Nature* **451**, 1090 (2008).
33. S. O. Rasmussen *et al.*, *J. Geophys. Res.* **111**, D06102 (2006).
34. See references 16 to 19 in the supplementary materials.

Acknowledgments: This article is dedicated to the memory of Prof. Y. Trzhcinski, who during the last months of his life made a big effort to establish the cooperation between the University of Oxford and Institute of Earth's Crust (IEC) in Irkutsk. We thank D. Sokolnikov and other "Arabica" members, E. Kozireva (IEC), V. Alexioglo, and V. Balaev from Lensk for their help during the fieldwork in Siberia; the Mongolian Speleological Society for their help with the fieldwork in Mongolia; J. Fritz and L. Zehnder (ETH Zürich) for preparing Fig. 1 and for assistance with XRD analyses, respectively; and C. Day, V. Ersek, L. Zanna, P. Holdship, O. Green, S. Wyatt, Y. Nakajima, P. Pousada Solino, J. Cox, S. Usher, M. Chung, and others from University of Oxford for the help with the laboratory work, administration and computing issues, obtainment of funding, and fruitful discussions. Supported by NERC Fellowship NE/G013829/1, Royal Society grant JP080831, and Russian Foundation for Basic Research joint grant 09-05-92605 KO_a.

Supplementary Materials

www.sciencemag.org/cgi/content/full/science.1228729/DC1
Materials and Methods
Supplementary Text
Figs. S1 to S16
Tables S1 to S3
References

13 August 2012; accepted 6 February 2013
Published online 21 February 2013;
10.1126/science.1228729

A Long-Lived Relativistic Electron Storage Ring Embedded in Earth's Outer Van Allen Belt

D. N. Baker,[1]* S. G. Kanekal,[2] V. C. Hoxie,[1] M. G. Henderson,[3] X. Li,[1] H. E. Spence,[4] S. R. Elkington,[1] R. H. W. Friedel,[3] J. Goldstein,[5] M. K. Hudson,[6] G. D. Reeves,[3] R. M. Thorne,[7] C. A. Kletzing,[8] S. G. Claudepierre[9]

Since their discovery more than 50 years ago, Earth's Van Allen radiation belts have been considered to consist of two distinct zones of trapped, highly energetic charged particles. The outer zone is composed predominantly of megaelectron volt (MeV) electrons that wax and wane in intensity on time scales ranging from hours to days, depending primarily on external forcing by the solar wind. The spatially separated inner zone is composed of commingled high-energy electrons and very energetic positive ions (mostly protons), the latter being stable in intensity levels over years to decades. In situ energy-specific and temporally resolved spacecraft observations reveal an isolated third ring, or torus, of high-energy (>2 MeV) electrons that formed on 2 September 2012 and persisted largely unchanged in the geocentric radial range of 3.0 to ~3.5 Earth radii for more than 4 weeks before being disrupted (and virtually annihilated) by a powerful interplanetary shock wave passage.

The magnetically confined radiation zones surrounding Earth were the first major discovery of the Space Age in 1958 (*1*–*4*). Long-term observations of these energetic particle populations have subsequently shown dramatic, highly dynamic changes of the outer Van